Effect of Iron Oxide Nanoparticles on Vascular Function and Nitric Oxide Production in Acute Stress-Exposed Rats

Short title

Iron Oxide Nanoparticles Affect Vascular Function and NOS activity

Silvia Líšková[1,2]*, Peter Bališ[1], Andrea Mičurová[1], Michal Kluknavský[1], Monika Okuliarová[3], Angelika Puzserová[1], Martin Škrátek[4], Ivan Sekaj[5], Jan Maňka[4], Pavol Valovič[1,6], Iveta Bernátová[1]*

[1] Institute of Normal and Pathological Physiology, Centre of Experimental Medicine, Slovak Academy of Sciences, Bratislava, Slovak Republic;
[2] Institute of Pharmacology and Clinical Pharmacology, Faculty of Medicine, Comenius University, Bratislava, Slovak Republic
[3] Department of Animal Physiology and Ethology, Faculty of Natural Sciences, Comenius University, Bratislava, Slovak Republic
[4] Institute of Measurement Science, Slovak Academy of Sciences, Bratislava, Slovak Republic
[5] Institute of Robotics and Cybernetics, Faculty of Electrical Engineering and Information Technology, Slovak University of Technology, Bratislava, Slovak Republic;
[6] Department of Nuclear Physics and Biophysics, Faculty of Mathematics, Physics and Informatics, Comenius University, Bratislava, Slovak Republic;

* Correspondence: Silvia Líšková, Institute of Pharmacology and Clinical Pharmacology, Faculty of Medicine, Comenius University, Sasinkova 4, 811 08 Bratislava, Slovakia (silvia.liskova@gmail.com) and Iveta Bernátová, , Institute of Normal and Pathological Physiology, Centre of Experimental Medicine, Slovak Academy of Sciences Sienkiewiczova 1, 811 09 Bratislava, Slovakia (iveta.bernatova@savba.sk)

Keywords

Vascular function; Acute stress; Iron oxide nanoparticles; Blood pressure; Nitric oxide; Polyethylene glycol

We investigated whether polyethylene glycol-coated Fe_3O_4 nanoparticles (IONs), acute stress and their combination modifies vascular functions, nitric oxide synthase (NOS) activity, mean arterial pressure (MAP) as well as hepcidin and ferritin H gene expressions in Wistar-Kyoto rats. Rats were divided into control, ION-treated rats (1 mg Fe/kg *i.v.*), repeated acute air-jet stress-exposed rats and IONs-and-stress co-exposed rats. Maximal acetylcholine (ACh)-induced and sodium nitroprusside (SNP)-induced relaxations in the femoral arteries did not differ among the groups. IONs alone significantly elevated the N^{ω}-nitro-L-arginine methyl ester (L-NAME)-sensitive component of ACh-induced relaxation and reduced the sensitivity of vascular smooth muscle cells to SNP. IONs alone also elevated NOS activity in the brainstem and hypothalamus, reduced NOS activity in the kidneys and had no effect in the liver. Acute stress alone failed to affect vascular function and NOS activities in all the tissues investigated but it elevated ferritin H expression in the liver. In the ION-and-stress group, NOS activity was elevated in the kidneys and liver, but reduced in the brainstem and hypothalamus *vs.* IONs alone. IONs also accentuated air-jet stress-induced MAP responses *vs.* stress alone. Interestingly, stress reduced ION-originated iron content in blood and liver while it was elevated in the kidneys. In conclusion, the results showed that 1) acute administration of IONs altered vascular function, increased L-NAME-sensitive component of ACh-induced relaxation and had tissue-dependent effects on NOS activity, 2) ION effects were considerably reduced by co-exposure to repeated acute stress, likely related to decrease of ION-originated iron in blood due to elevated decomposition and/or excretion.

Introduction

The last decade of investigations of metal nanoparticles (NPs), including superparamagnetic iron oxide nanoparticles (IONs), have revealed their potential for various biomedical applications, from magnetic resonance imaging contrast agents including detection of bacteria or viruses to drug delivery systems and the usage of magnetic hyperthermia in cancer treatment (Andrade *et al.* 2020, Poller *et al.* 2018). However, the properties and biological effects of IONs vary depending on their shape, size, surface modification, *etc*. In general, smaller nanoparticles (1–20 nm) seem to enter and exit the cell more efficiently and infiltrate organs better than larger ones, spherical NPs are less toxic than rod-shaped ones and positively charged NPs exhibit much higher rates of endocytosis and remain in the cell longer than negative or neutrally charged ones (Oh and Park 2014).

Bare IONs are toxic mainly due to the induction of haemolysis, oxidative stress and DNA breakdown (Andrade *et al.* 2020, Dalzon *et al.* 2020). Thus, various coatings have been developed to reduce ION cytotoxicity. Hydrophilic polymer polyethylene glycol (PEG) is a neutral biocompatible polymer, which improves the dispersion of IONs in water, improves the biodistribution of NPs in an organism and increases blood circulation time (Yoffe *et al.* 2013). The PEGylation of nanoparticles has also been shown to reduce hemotoxic effects, haemolysis, liver uptake and immunogenicity (Lee *et al.* 2005, Suk *et al.* 2016). Intravenous application is the common route for IONs in therapeutic applications, such as drug delivery, nanocarriers and diagnostic tools (Dukhinova *et al.* 2019). The main ways to eliminate IONs are through renal and hepatic excretions (Almeida *et al.* 2011, Longmire *et al.* 2008). However, the iron released from decomposed IONs can also enter cellular iron metabolism (Poller *et al.* 2018) and thus can affect iron homeostasis. Elevated iron levels results in the elevation of hepatic hepcidin release, which is the main regulator of iron homeostasis as well as in the elevation of ferritin synthesis, which is a main iron-storage protein, in order to recover optimal iron concentrations

in the tissues (De Domenico *et al.* 2010). In addition, ferritin levels can be altered in oxidative stress conditions (Torti and Torti 2002) which is often induced by NPs.

Endothelium, the inner monolayer of blood vessels, produces various substances collectively termed endothelium-derived factors, which modulate vascular functions and thus blood pressure (Bernatova 2014). Endothelial cells are directly exposed to IONs when administered intravenously. Su *et al.* observed ION uptake to endothelial cells *in vitro*, in which IONs were located in the cytoplasm (Su *et al.* 2012). ION uptake was also detected in the endothelial cells of cerebral arteries *in vitro* in which IONs induced the release of reactive oxygen species, DNA damage and autophagy (Kenzaoui *et al.* 2012). ION accumulation in endothelial cells can modify the function of the endothelium and/or vascular wall by activating inflammation, disrupting cellular respiration and inducing oxidative stress and apoptosis (Yarjanli *et al.* 2017) and altering nitric oxide (NO) production. Astanina *et al.* observed reduced NO production in cultured endothelial cells after their incubation with recommended doses of IONs approved for medical purposes (Astanina *et al.* 2014). Zhu *et al.*, in contrast, observed that IONs generated oxidative stress, increased NO production and induced the loss of mitochondria membrane potential and apoptosis in endothelial cell cultures (Zhu *et al.* 2010). As IONs in concentrations relevant for *in vivo* applications can affect endothelial cells, their influence on the endothelium and vascular wall functions must be investigated to understand their possible cardiovascular side effects in humans (Astanina *et al.* 2014).

Stress is considered a risk factor associated with the development of various chronic diseases, including cardiovascular diseases. Despite the variability of stressors and their effects on organisms, sudden stressors can activate the autonomic nervous system, which is associated with increased blood pressure (BP) and heart rate (HR). On the other hand, NO is a major depressor factor that attenuates BP increases via attenuation of sympathetic nervous system (SNS) activation along with the renin-angiotensin-aldosterone system (Kumagai *et al.* 2012). Vascular and/or endothelial function can also be altered by stress (Puzserova and Bernatova

2016). Despite considerable differences between *in vitro* and *in vivo* studies that have investigated the influence of stressors on the production of endothelium-derived factors (Bernatova 2014), endothelium-derived NO has been suggested as a stress-relieving molecule (Stefano *et al.* 2006). Thus, stress may be a factor that considerably modifies the effect of treatment via modulation of vascular functions and feedback effect on the autonomic nervous system, as demonstrated by acute pharmacological adrenalectomy (Bencze *et al.* 2020). In addition, excessive NO production due to the activation of inducible NO synthase (NOS) contributes to vascular hypo-reactivity, reduces systemic resistance and decreases blood pressure (El Hadi *et al.* 2020).

In this study, we used acute air-jets to induce stress reactions associated with prominent BP increase ~~during air jet~~ to investigate the modulatory effect of repeated acute stress on ION administration. Air-jet stress results in psycho-emotional stress, which causes a characteristic defence reaction with increases in BP, HR and renal sympathetic nerve activity (Bernatova *et al.* 2016, Kanbar *et al.* 2007, Yamazato *et al.* 2006). It is well known that acute stress alters neurohumoral mechanisms, which leads to changes in vascular function and thus stress alters blood flow and distribution (Wang *et al.* 2005). All these factors should be taken into account during IONs application in humans.

The femoral artery is an important branch of the iliac artery that irrigates lower-limb skeletal muscles and peripheral tissues. It is a unique blood vessel with long conduction, high-flow resistance and a striking relevance for medical interventions (Mewissen 2005). Femoral artery tone regulation depends on endothelium-derived relaxing and contracting factors (Bencze *et al.* 2015, Dobias *et al.* 2016, Líšková *et al.* 2007), thus representing an ideal artery for studying vascular responses in various experimental approaches. One such approach involve the inhibition of NOS leading to the impairment of NO release, which in turn may unmask the effect of endothelium-derived contracting factors (EDCFs) (Liskova *et al.* 2011). This is of particular importance because the application of N^{ω}-nitro-L-arginine methyl ester (L-NAME

allows the assessment of the L-NAME-sensitive component of concentration-response curves induced by acetylcholine (ACh). The L-NAME-sensitive component has NO-dependent and EDCFs-dependent part and thus after L-NAME application the isolated femoral arteries react with enhanced concentration-dependent contractions (Liskova *et al.* 2011) or impaired concentration-response curves of endothelium-dependent ACh-induced relaxations (Puzserova *et al.* 2013). Due to intravenous administration of IONs in clinical applications, it is of great importance to study the effect of IONs on endothelial cells as nanoparticles *per se* or iron released from them may penetrate the vascular wall and thus change vascular functions. Furthermore, it is reasonable to investigate the joint influence of acute stress on vascular function and NOS activity as diseases, hospital environments and/or intravenous applications of IONs are always associated with certain levels of stress in patients.

Thus, in this study we investigated the effect of *i.v.* administration of IONs on vascular functions of the femoral arteries of normotensive rats, NOS activity in the tissues (kidneys, liver, brainstem and hypothalamus) and on BP at rest (~100 min-post infusion, at the end of the experiment). We also investigated acute stress-induced BP and HR responses in ION-treated rats because of the possibility of stress conditions during the use of IONs in medical practice. In addition, we determined the effect of IONs on gene expression of hepcidin (HAMP) and ferritin (FTH1) in the liver and kidneys (involved in excretion of IONs) as well as the effect of repeated acute stress on ION-originated iron content in these organs and blood.

Materials and Methods

Animals and treatment

All the procedures used in this study were approved by the State Veterinary and Food Administration of the Slovak Republic in accordance with the European Union Directive 2010/63/EU.

Wistar-Kyoto (WKY) male rats 12–16 weeks old, n = 6–7 per group, were used in this study. Rats were housed under standard conditions at 22–24°C in a 12-h light/dark cycle and fed with pelleted diet Altromin formula 1324, variant P (Altromin Spezialfutter, Lage, Germany) and tap water *ad libitum*.

A day before the experiment, all rats had two catheters implanted under 2.5–3.5% isoflurane anaesthesia, as described previously (Behuliak *et al.* 2013). All rats were also pre-treated with meloxicam (Meloxidolor, Le Vet Beheer B.V., Oudewated, Nederland) at 2 mg/kg *i.m.* before surgery to prevent post-surgical pain. Fine-bore polyethylene catheters (Smiths Medical International Ltd, Kent, UK) were inserted into the left carotid artery (internal diameter 0.58 mm) to determine BP and HR and the jugular vein (internal diameter 0.28 mm) for *i.v.* administration of IONs (suspended in saline) or saline (in control and stressed rats), respectively. Catheters were exteriorised in the interscapular region, and rats were allowed to recover from anaesthesia for approximately 20–24 h.

Rats were divided into four groups: control (Cont), ultra-small superparamagnetic iron oxide (Fe_3O_4) nanoparticle (ION)-treated rats (IONs), repeated acute air-jet stress-exposed rats (Str) and rats co-exposed to IONs and repeated air-jet stress (IONs + Str). Control and stressed rats were given 10-min infusions of saline starting approximately 30 min from the beginning of BP recording (Figure 1). IONs and IONs + Str rats were given 10-min infusions of PEG-coated IONs. Commercially available PEG-coated IONs were purchased from Sigma-Aldrich (Bratislava, Slovakia, cat. No. 747408). IONs concentration was 1 mg Fe/ml and they were dispersed in water. The size of IONs confirmed by the transmission electron microscope was 28–32 nm, the zeta potential was -12 mV, polydispersity index was 0.1 and the hydrodynamic size was about 45 nm (declared by the manufacturer). IONs were autoclaved at 121°C for 30 min and before *i.v.* application they mixed with sterile saline to reach a final dose of 1 mg of Fe/kg of body weight. Properties of IONs before their administration to rats and their presence

in the tissues (proven by bio-magnetometric method) are shown in other study (Skratek *et a*l. 2020, unpublished results).

The experiments were performed in a quiet room to avoid any non-specific stimuli affecting BP and HR, which were recorded with the sampling rate of 1 kHz. During the experiments, the conscious rats were placed in a plastic box with dark walls and a transparent lid 27 × 14 × 9 cm in size, which allowed the rats free movement. An arterial catheter was attached to the BP-recording device PowerLab system (ADInstruments, Bella Vista, Australia), and BP was allowed to stabilise for at least 15 min. BP and HR were recorded during the entire experiment, basal mean arterial pressure (MAP) and HR were calculated as the average values of a 200-sec segment between 16–20 min of the recording and end MAP and HR were calculated as the average values of a 200-sec segment between 138–142 min of the experiment. The peak values of MAP and HR were also calculated during each air-jet (AJ) session as the maximal values of the given variable during air-jet compared with the average pre-AJ value determined during 200-sec segments preceding the corresponding AJ session (Figure 1). Repeated acute AJ stress was produced by a 5-sec pulse of air at the forehead of the rat in the Str and IONs + Str groups as described previously (Bernatova *et al.* 2016, Nakamoto *et al.* 2007). Each rat in these two groups was exposed to three sessions of 5-sec AJ: 1) 10 min before the infusion, 2) 10 min after the infusion and 3) 90 min after the infusion. Variable time points were chosen to maintain the unpredictability of the stressor (Bernatova *et al.* 2016). BP recordings were transformed into a MATLAB® environment for further analysis. MAP was calculated as MAP = diastolic BP + 1/3 (systolic BP – diastolic BP) (Bernatova *et al.* 2016).

At the end of the protocol, rats were exposed to brief CO_2 anaesthesia and decapitated within 5 min of the final MAP recording. Trunk blood for determination of IONs was collected into Eppendorf test tubes and kept at -80 °C. The NOS activity was determined in fresh tissue homogenates of the brain stem, hypothalamus, kidney and liver. The remaining parts of dissected kidneys and liver were frozen in liquid nitrogen and kept at -80 °C for further

analyses. Femoral arteries were stored in fridge at 4 °C and used the same day for vessel myography.

Plasma corticosterone

Plasma corticosterone was determined in 50 µl blood samples collected from the carotid artery (before the end of experiment) into ethylenediaminetetraacetic acid-coated test tubes and centrifuged for 10 min (850 g, 4°C). Plasma samples were stored at -80°C until further analysis. Plasma corticosterone levels were determined using the Corticosterone Rat/Mouse ^{125}I radioimmunoassay kit (DRG Instruments GmBH, Germany), according to the manufacturer's instructions. All samples were measured in a single assay with the intra-assay variation coefficient of 4%. The assay sensitivity was 6.3 ng/ml.

Nitric oxide synthase activity

Nitric oxide synthase (NOS) activity was determined in 20% of fresh tissue homogenates (w:v) of the brainstem, hypothalamus, kidneys and liver as described previously with minor modifications (Puzserova *et al.* 2013). Briefly, tissues were collected into ice-cold buffer (0.05 mol/l Tris–HCl, pH 7.4, containing 1% protease inhibitor cocktail [104 mmol/l of 4-(2-aminoethyl)benzenesulfonyl fluoride, 80 mmol/l aprotinin, 4 mmol/l bestatin, 1.4 mmol/l of E-64, 2 mmol/l leupeptin and 1.5 mmol/l of pepstatin A]). The tissues were then immediately homogenised using an Ultra-Turrax homogeniser at 4°C and centrifuged (4°C, 10 min, 3000 g). After centrifugation, NO synthase activity was determined in the supernatants by the conversion of [3H]-L-arginine (specific activity 5 GBq/mmol, ~100,000 dpm, ARC, St. Louis, MO, USA) to [3H]-L-citrulline in the presence of 50 mmol/l Tris/HCl, pH 7.4 (containing 10 µmol/l L-arginine, 5 µg/ml calmodulin, 0.5 mmol/l β-NADPH, 0.6 mmol/l tetrahydrobiopterin, 4 µmol/l flavin adenine dinucleotide, 4 µmol/l flavin mononucleotide, 1 mmol/l Ca^{2+} and 1 mmol/l Mg^{2+}) in a total volume of 100 µl. After 20 min of incubation at 37°C, the reaction was stopped by

adding 1 ml of ice-cold stop solution (containing 20 mmol 4-(2-hydroxyethyl)-1-piperazineethanesulfonic acid, pH 5.5, 1 mmol/l L-citrulline, 2 mmol/l EDTA and 2 mmol/l EGTA). Then 1 ml of the mixture was applied to 1.5 ml Dowex 50WX-8 columns (Na^+-form). [3H]-L-citrulline was eluted by 1.5 ml of deionised water and determined by liquid scintillation counting (TriCarb, PerkinElmer). NO synthase activity was expressed as pkat per gram of protein. The protein concentration was determined using the Lowry method.

Determination of vascular functions

Isolated and cleaned fresh femoral arteries with intact endothelium were cut into segments and placed in a Mulvany-Halpern isometric myograph (Dual Wire Myograph system *410A*, Danish Myo Technology A/S, Aarhus, Denmark). The myograph chambers were filled with modified Krebs-Henseleit solution (in mmol/l: 119 NaCl, 4.7 KCl, 1.17 $MgSO_4.7H_2O$, 25 $NaHCO_3$, 1.18 KH_2PO_4, 0.03 Na_2EDTA, 2.5 $CaCl_2.2H_2O$, 5.5 glucose, 37°C, pH 7.4) and bubbled with 95% O_2 and 5% CO_2. The inner arterial diameter of femoral arteries was set to 90% of the diameter predicted for the pressure of 100 mmHg in the wire myograph. After 30 min of stabilisation, the arteries achieved their basal tones. To test the viability of isolated arteries, the arteries were incubated in a depolarising solution (125 mmol/l K^+, NaCl was exchanged for an equimolar concentration of KCl) for 2 min. After being washed out, the experimental protocol was carried out as described in another study (Puzserova *et al.* 2013). Briefly, after the washing and stabilisation of the basal tone, 5-HT-induced contraction (10^{-6} mol/l) was determined. It was followed by determination of the total endothelium-dependent ACh-induced relaxations by cumulatively adding ACh at the final concentrations 10^{-9} to 10^{-5} mol/l. After 20 min of washing out, the same approach was applied again in the presence of the non-specific NO synthase inhibitor L-NAME (3.10^{-4} mol/l, 30 min pre-incubation) to determine 5-HT contraction in the presence of NO synthase inhibitor as well as the NO-independent component of endothelium-dependent relaxation. After repeating washing, the third

concentration-response curve was performed by cumulatively adding exogenous NO donor (SNP) in concentrations of 10^{-9} to 10^{-5} mol/l to determine the endothelium-independent relaxations produced by exogenous NO on VSMCs.

Pharmacodynamic characteristics – *i.e.* half-maximal effective concentration (EC_{50}, expressed as -log mol/l) and maximal relaxation (E_{max}, expressed as a percentage of pre-constriction) – were calculated for each ACh- and SNP-induced concentration-response curve according to the Hill equation using the fitting model described in another studies (Liskova *et al.* 2014, Liskova *et al.* 2010). The L-NAME-sensitive component of ACh-induced relaxation was calculated as the difference between the AUC of total ACh-induced relaxation and AUC of the NO-independent ACh-induced relaxation, *i.e.* $AUC_{L\text{-}NAME\text{-}sensitive} = AUC_{TotalACh} - AUC_{NO\text{-}independent}$.

All chemicals used in the study were obtained from Sigma-Aldrich (Bratislava, Slovakia) unless stated otherwise.

Determination of the ION-originated iron content

After dissection, the tissues were cleaned out of the connecting tissue, washed out of blood in the saline solution and dried of saline solution using filtration paper. Trunk blood was collected into Eppendorf test tubes. Tissues as well as blood were frozen in the liquid nitrogen and kept at -80°C until further analyses. Before determination of relative iron content, tissue samples were mounted on 18 cm long and 0.2 mm in diameter copper wire. Blood samples were prepared as described previously and 10 µl was dropped on paper (Kluknavsky *et al.* 2020). Then samples were vacuum dried for 1 hour, placed in plastic straw and the magnetic characteristics of the samples were measured by a Quantum Design SQUID magnetometer MPMS-XL 7AC. Determination of ION-originated Fe content in tissue and blood samples was done by measuring their hysteresis curves (M vs H dependence) measured at the temperature

of 300 K and up to 1 T applied field. The iron content in the blood, liver and kidneys of IONs and IONs + Str groups was determined using the following relation:

$$c\left[\frac{\mu g_{Fe}}{g}\right] = \frac{M_S' * m_{Fe}}{M_{IONs} * m_s} * 10^6$$

Where c is the IONs-originated Fe content in the sample, M'$_S$ is sample magnetization (at 1 T) after subtraction of magnetization of the control tissue, m_s is the mass of the sample, m_{Fe} is the mass of iron in 10 µl of IONs, M_{IONs} is magnetization of ION dispersion measured at temperature 300 K and magnetic field 1 T. At this conditions, the method determines only IONs-originated Fe because magnetic characteristics of biogenic iron present in the tissue differs from those of nanoparticle dispersion of PEGylated IONs and magnetisation of biogenic iron was subtracted.

Determination of the gene expression

The gene expression levels of hepcidin (HAMP, NM_053469.1) in the liver and ferritin heavy chain 1 (FTH1, NM_012848.2) in the liver and kidneys as well as expression of ß-actin (housekeeping gene, NM_031144.3) were determined after mRNA isolation using a real-time quantitative polymerase chain reaction (RT-qPCR) as described previously (Kluknavsky *et al.* 2020). Gene-specific primers were designed using the PubMed program (Primer-BLAST) and database (Gene). The gene expressions were considered as the ratio of the given gene's expression to β-actin expression. The following primer pairs and melting temperatures were used to determine selected genes: *HAMP* (forward - CTA TCT CCG GCA ACA GAC GAG, reverse - TGT CTC GCT TCC TTC GCT TC, 60°C), FTH1 (forward - ACG TCT ATC TGT CCA TGT CTT GTT, reverse - GAA GAT TCG TCC ACC TCG CT, 60°C), β-actin (forward - CTC TGT GTG GAT TGG TGG CT, reverse - CGC AGC TCA GTA ACA GTC CG, 59°C).

Statistical analysis

Statistical analysis was performed by two-way ANOVA (with IONs and stress as the independent factors) or two-way ANOVA for repeated measures ANOVA and Student's t-test, where appropriate. ANOVA analyses were followed by the Bonferroni post-hoc test, except the analysis of the release of EDCFs in the IONs group after ACh-administration, which was analysed by one-way ANOVA and Dunnett's test. The values were found to significantly differ when $p < 0.05$. The data were presented as mean ± standard error of the mean (SEM). GraphPad Prism 5.0 (GraphPad Software, Inc., San Diego, CA, USA) was used for the statistical analyses.

Results

Mean arterial pressure, heart rate and plasma corticosterone

The mean arterial pressure (MAP) and HR of all rats at the beginning of the experiment were 132 ± 2 mmHg and 330 ± 6 bpm (n = 27), and no significant differences among the groups in these parameters were observed. MAP was reduced significantly at the end of the experiment *vs.* basal values in rats co-exposed to IONs and air-jet stress (IONs + Str) (Figure 2A). HR was reduced significantly in control (Cont), ION-treated rats (IONs) and acute air-jet stress-exposed rats (Str) groups *vs.* the respective basal values (Figure 2B).

~~MAP in the Cont, Str and IONs groups at the end of the experiment was 102 ± 4%, 99 ± 1% and 99 ± 2% of basal MAP, respectively, which were not significantly altered compared to basal MAP within each group. The MAP of rats in the IONs + Str group decreased significantly at the end of the experiment to 88 ± 4% of basal MAP ($p < 0.02$). HR in the Cont, Str and IONs groups at the end of the experiment was 89 ± 3%, 90 ± 2% and 88 ± 2% ($p < 0.05$ *vs.* basal for all), respectively. HR in the IONs + Str was 94 ± 2% of basal HR (n.s.).~~ The peak values of MAP and HR during the second and the third air-jet (AJ) sessions were calculated as a percentage change of the response found during the first AJ (Figure 2C, D). ANOVA analysis

showed that IONs significantly increased the pressor responses to the stress produced by air-jet (AJ2 and AJ3) when evaluated as the main effect of the IONs + Str co-application ($F_{(1,10)}$ = 14.07, $p < 0.004$), without the significant changes in peak HR responses.

Plasma corticosterone was significantly elevated in rats exposed to stress when determined as the main effect of stress in both stress-exposed groups ($F_{(1,20)} = 9.6$, $p < 0.006$ *vs.* unstressed rats), while IONs did not affect this parameter (Figure 3).

NO synthase activity

In the kidneys, NOS activity decreased in the IONs group by about 22% ($p < 0.03$) *vs.* controls (Figure 4A), while no changes were found in the liver (Figure 4B). ION administration elevated NOS activity in the hypothalamus and brainstem by 34% ($p < 0.03$) and about 62% ($p < 0.01$), respectively, compared to the controls (Figure 4C, D). In the IONs + Str group, NOS activity was significantly elevated in the kidneys 40% ($p < 0.01$) and liver 20% ($p < 0.05$) and reduced in the brainstem 55% ($p < 0.001$) and hypothalamus 38% ($p < 0.001$) *vs.* the IONs group. Stress alone had no effect on NOS activity in any tissue investigated vs. control Similarly, no differences in NOS activity were found between Str and IONs + Str groups (Figure 4).

Contraction responses of the femoral arteries

The mean internal diameter of all arterial segments used in this study was 717 ± 7 μm and did not differ significantly among the groups. The maximal depolarisation-induced contractions produced by the high concentration of potassium (125 mmol/l K^+) in Cont, IONs, Str and IONs + Str were 8.24 ± 1.27, 7.09 ± 1.25, 9.58 ± 0.57 and 9.31 ± 1.14 mN/mm, respectively, and no significant differences were observed among the groups.

Maximal serotonin (5-HT)-induced contractions in the absence of ~~N^{ω}-nitro-L-arginine methyl ester~~ (~~L-NAME~~) were similar among the groups (Figure 5). Pre-incubation of the

arteries with L-NAME significantly enhanced the 5-HT-induced contraction of femoral arteries in the Cont, Str and IONs + Str groups compared to the 5-HT-induced contraction in absence of L-NAME by approximately 36%, 38% and 18% ($p < 0.05$ for all groups), respectively. A correspondingly significant increase was not found in the IONs group.

Relaxation responses of the femoral arteries

The acetylcholine (ACh)-induced and sodium nitroprusside (SNP)-induced concentration-response curves of 5-HT-precontracted femoral arteries are shown in Table 1 and Figure 6.

Maximal ACh-induced relaxations (E_{max}) were not altered by stress, IONs or their joint application *vs.* control (Table 1, Figure 6A).

L-NAME significantly reduced ACh-induced relaxation ($F_{(1,21)} = 29.3$, $p < 0.0001$) *vs.* relaxations in absence of L-NAME (Figure 6B) and allowed the calculation of $E_{max\ L\text{-}NAME}$, which was significantly reduced in the IONs group compared to total relaxation (*i.e.* E_{max}). In addition, $E_{max\ L\text{-}NAME}$ for the IONs + Str group was significantly elevated compared to the IONs group (Table 1). $EC_{50\ L\text{-}NAME}$ was shifted to higher concentrations in all groups investigated *vs.* EC_{50} without L-NAME (Table 1). The L-NAME-sensitive component, calculated from the E_{max} values as a difference between E_{max} and $E_{max\ L\text{-}NAME}$, increased in the femoral arteries of the IONs group, but it returned to the level present in the Cont group in the femoral arteries of rats co-exposed to IONs + Str (Table 1). The area under the curve (AUC) calculated from the cumulative concentration response curves to ACh in the presence of L-NAME (*i.e.* the L-NAME-resistant component) was significantly reduced while the L-NAME-sensitive component was significantly elevated in ION-treated rats *vs.* the respective control values. Moreover, the L-NAME-sensitive component of the IONs + Str group was significantly reduced compared to that of the IONs group (Figure 6D). Pre-treatment of the arteries with the L-NAME led also to the significant reduction of relaxations at the highest ACh-concentration

only in the IONs group *vs*. the maximal relaxation in this group at lower ACh-concentration (Figure 6B), suggesting the release of EDCFs.

The maximal relaxations induced by cumulative concentrations of the exogenous NO donor SNP were not altered significantly in any group *vs.* the control group (Table 1, Figure 6C). The sensitivity of the femoral arteries to SNP expressed as EC_{50} was significantly decreased in the IONs and IONs + Str groups *vs.* the control group (Table 1).

IONs-originated iron contents

ION-originated iron was present mainly in whole blood, lower amounts were present in the liver and kidneys (Figure 7). In blood (Figure 7A) and liver (Figure 7B), stress reduced IONs-originated iron content by approximately 92% and 69 % vs. IONs group ($p < 0.04$ for both). On the other hand, ION-originated iron content increased significantly in the kidneys (Figure 7C) by 296% ($p < 0.03$).

Gene expressions

Expression of the HAMP gene in the liver was significantly elevated when determined as the main effect of ION-administration ($F_{(1,17)} = 6.00$, $p < 0.03$) (Figure 8A). Despite tendency of higher FTH1 gene expression in the liver of ION-treated rats was observed, this did not reach statistically significant effect vs. the control group. In contrast, stress significantly elevated FTH1 gene expression in the liver by 122% vs. control ($p< 0.006$, Figure 8B). In the kidneys, no changes in the FTH1 gene expression were observed (Figure 8C).

Discussion

This study investigated the effect of intravenously administered ultra-small PEG-coated IONs and its interaction with acute stress on vascular function, NOS activity, BP and HR and expression of HAMP and FTH1 genes in Wistar-Kyoto rats (WKY). The main findings are that

IONs modified the vascular function of the femoral arteries. In these arteries IONs 1) increased the L-NAME-sensitive component of ACh-induced relaxations, 2) decreased the sensitivity of the vascular smooth muscle cells (VSMCs) to exogenous NO and 3) prevented the increase of 5-HT-induced contractions after L-NAME, and 4) induced EDCFs release in L-NAME pre-treated arteries. IONs also enhanced NOS activity in the brainstem and hypothalamus and reduced NOS activity in the kidneys. Notably, the combination of IONs with repeated acute air-jet stress had no effects on the overall endothelium-dependent relaxations but altered NOS activity in the tissues and IONs-originated iron content in blood and tissues compared to IONs alone. In addition, in IONs + Str group IONs increased AJ-induced pressor responses, but decreased MAP determined ~100-min post-infusion compared to basal value, which was not found in any other group of rats. In the groups of rats exposed to acute air-jet stress, we found increased concentrations of plasma corticosterone, which are in line with previous results evaluating the effects of this stressor (Stojićić *et al.* 2008, Wsol *et al.* 2020). These data prove that the intensity and duration of the stressor were effective in inducing stress response.

Various studies have examined the cardiovascular effects of IONs. In human cardiac microvascular endothelial cells, IONs have not altered the viability, membrane integrity or inflammation markers of cells (Sun *et al.* 2011). In Sprague-Dawley rats with IONs administered once per day for 7 days, IONs have reduced infarct size, elevated superoxide dismutase activity and reduced oxidative stress and the activities of several enzyme markers of heart damage (Xiong *et al.* 2015). On the other hand, the *i.v.* administration of IONs in mice has led to oxidative stress, increased levels of reactive oxygen species and superoxide dismutase activity in the heart (Baratli *et al.* 2013, Bostan *et al.* 2016). In humans, hypotension and vasodilatation have been side effects of certain IONs when administered as contrast agents to improve magnetic resonance imaging (Wang 2011). Iversen *et al.* reported a transient decrease in the MAP course of 12–24 h after introducing polyacrylic acid (PAA)-coated γ-Fe_2O_3 nanoparticles (Iversen *et al.* 2013). We expected that exposure to acute stress would increase

MAP and prevent possible MAP reduction after ION application. However, in our study, IONs and stress, respectively, did not alter MAPs at the end of the experiment compared to the basal MAPs. Similarly, Nunes *et al.* found no alterations in the MAP of rats after the infusion of three types of manganese ferrite–based magnetic NPs (Nunes *et al.* 2014). ~~Surprisingly, co-exposure of ION-treated rats to acute stress in this study resulted in a significant MAP decrease at the end of the experiment compared to basal MAP.~~

Next, we investigated alterations of vascular function. This is, to the best of our knowledge, the first study that determined L-NAME-sensitive and L-NAME-resistant components of endothelium-dependent ACh-induced relaxation after ION administration. Regarding vasorelaxation, NO is the master of endothelium-dependent relaxation (Bernatova 2014), the lack of NO is associated with reduced vasorelaxation and BP elevation (Rauchová *et al.* 2005). However, the effect of stress on vasculature varies depending on the model, duration and intensity of stress as well as on artery type (Puzserova and Bernatova 2016). In this study, we found that IONs alone as well as interacting with acute stress significantly reduced the sensitivity of VSMCs to the exogenous NO donor SNP (expressed as decreased EC_{50} in SNP-induced relaxations) compared to the control group without changes in maximal SNP-induced relaxation. The effect of stress alone was not significant in this parameter. This suggests that IONs reduced the sensitivity of VSMCs to NO. The reduction of sensitivity to NO may result from the deleterious effect of IONs on VSMCs and/or from elevated NO release from the endothelium. We found the greatest L-NAME-sensitive component of ACh-induced relaxation in ION-treated rats which might result from greater NO bioavailability and/or from elevated ION-induced EDCFs release. As we also found elevated ION-induced superoxide release in the tissues of rats, including the aorta (Škrátek e*t al*. 2020), the elevated EDCFs release is plausible in the ION-treated rats. The release of EDCFs was visible in this study at the end of ACh-concentration-response curves (in the presence of L-NAME) in ION-treated rats as the decrease of ACh-induced relaxation at the highest concentration compared to maximal ACh-induced

relaxation in the given group (achieved at lower ACh concentration, Fig. 6B) and it was attenuated by exposure to repeated acute stress. Such a release of EDCFs is common in spontaneously hypertensive rats or in aged WKY supposedly due to a lack of inhibitory influence of NO on the release of the EDCFs (Liskova *et al.* 2011, Puzserova *et al.* 2013). On the other hand, application of L-NAME failed to elevated 5-HT-induced vasocontractions in ION-treated rats. This finding, again points to elevated NO bioavailability in the ION-treated rats because the inhibitory effect of NO on 5-HT and noradrenaline-induced contractions in the femoral arteries has been shown previously in non-stressed rats (Liskova et al. 2011, Puzserova et al. 2013) as well as in stressed ones (Slezak et al. 2014). Thus, the changes in vascular wall function after IONs application are complex and additional, more specific, experiments are needed to identify the exact mechanism responsible for alterations in vascular function in rats after administration of PEG-coated IONs.

The mechanism of functional changes in vasculature after *i.v.* administration of IONs lacks attention in the literature. Recent studies have shown no direct effects of increasing concentrations of Fe_3O_4 nanoparticles (size 50–100 nm, *in vitro* cumulative administration) on the contractility of human mesenteric arteries (Vukova *et al.* 2016). Nunes *et al.* found mild relaxation of isolated rat aortic rings using cumulative *in vitro* application of bare manganese ferrite-based magnetic NPs (Nunes *et al.* 2014). Iversen *et al.* reported that *in vitro* incubation of small mesenteric arteries from healthy mice with PAA-coated γ-Fe_2O_3 nanoparticles reduced maximal contractions in response to increasing concentrations of noradrenaline (Iversen *et al.* 2013). Furthermore, the application of PAA-coated γ-Fe_2O_3 nanoparticles for 24 h *in vivo* reduced the maximal contractions of small mesenteric arteries to noradrenaline in mice, which gradually disappeared and was absent on the 7^{th} day of nanoparticle exposure (Iversen *et al.* 2013). The important finding of our study is that exposure to acute repeated stress and co-exposure to IONs and stress failed to aggravate the vascular functions of WKY rats. In fact, stress reduced ION-induced alterations (except for reduced sensitivity of VSMCs to exogenous

NO), which may result from the high blood flow-induced shear stress and alterations of NO and/or EDCFs release ~~by endothelial NOS~~ during acute stress [for review see (Puzserova and Bernatova 2016)]. However, it may also result from a reduction of IONs amount in blood of rats co-exposed to stress as ~~what~~ we have shown in this study. It is worthy to mention that the vascular effects of NPs of different chemical moiety investigated in various experimental conditions *(e.g.* route of administration, dose, duration of treatment, various pre-contraction agents, artery type, *etc.*) may affect different physiological and molecular mechanisms (Courtois *et al.* 2010).

In our study, in addition to vascular functions, we investigated NOS activity in the hypothalamus, brainstem and kidneys, since those structures affect BP regulation in both normal and stressed conditions. We found augmented NOS activity in the brainstem and hypothalamus but decreased NOS activity in the kidneys of ION-treated rats. The enhancement of NOS activity in brain structures could lead to sympathoinhibition (Kumagai *et al.* 2012). Kishi showed that NO derived from the overexpression of endothelial NOS in the rostral ventrolateral medulla in the brainstem caused sympathoinhibition (Kishi 2013). Next, within the hypothalamic paraventricular nucleus, NO generated by neuronal NO synthase played a major constitutive role in suppressing ongoing renal sympathetic activity and regulating arterial pressure in Wistar rats (McBryde *et al.* 2018). As documented previously, a well-known cross-link exists between the brain (*i.e.* SNS and/or CNS) and kidney (*i.e.* the renin-angiotensin-aldosterone system) as well as NO and kidney functions in the regulation of BP (Kishi 2013, McBryde *et al.* 2018, Pecháňová *et al.* 2006, Drábková *et al.* 2020). Thus, we assume that enhanced NOS activity in the given brain structures may lead to sympathoinhibition possibly manifested in decreased NOS activity in the kidneys of ION-treated rats, leading to maintenance of unaltered levels of BP. Interestingly, in the IONs + Str group, stress blocked the increase of NOS activity in both brain structures and prevented the decrease in NOS activity in the kidneys compared to the IONs group. We assume that the simultaneous influence of two independent

stressors could cause dysregulation of BP regulatory systems, which led to a temporary decrease of the resting MAP in the IONs + Str group. In addition, the decrease of MAP at rest in the IONs + Str group may, at least partially, results from elevated NOS activity in the liver. It is well known that the high production of inducible NOS-derived NO and/or other vasodilators in the liver leads to reduced systemic vascular resistance and hypotension (El Hadi *et al.* 2020). Thus, our results suggest that IONs have a complex effect on BP regulation, which includes the hypothalamus, brainstem, kidneys, liver and vasculature. Our findings also point to the importance of acute stress during ION-administration that might reduce the amount of IONs in circulation. In particular, IONs *i.v.* administration resulted in greater BP rise after air-jet stress (AJ2 and AJ3, Figure 2C) that may alter the blood flow leading to elevated IONs decomposition and/or iron storage in the liver and to the decrease of IONs-originated iron in blood of IONs + Str rats. Our findings of elevated HAMP gene expression suggest elevated systemic iron levels in IONs-exposed rats. Despite the organism lacks regulated mechanism of excretion of iron itself, IONs bigger than 6 nm can be excreted via hepatobiliary clearance. Furthermore, if IONs are decomposed to the particles smaller than 6 nm, renal excretion of IONs can also participate in reduction of ION-derived iron in blood (Zhang *et al.* 2016). Because we did not measured IONs in urine and feces, we cannot exclude any of these routes.

Conclusions

Collectively, our results indicate that single *i.v.* administration of a low dose of PEG-coated IONs altered mechanisms of vascular wall function ~~of increased NO and/or EDCFs release in vascular wall~~ of femoral arteries, as manifested by enhanced L-NAME-sensitive component of ACh-induced relaxation, by the reduction of sensitivity to exogenous NO and by the absence of augmentation of 5-HT-induced contractions after NOS inhibition. These effects of IONs were ~~absent~~ reduced when rats were exposed also to repeated acute stress despite acute stress itself having no effect on these parameters. In addition, ~~joint~~ exposure of ION-treated rats to

repeated acute stress reduced ION-originated iron in blood and liver, affected NOS activity and altered the mechanisms of BP regulation, resulting in enhanced pressor responses to stress, but reduced MAP at rest. Our findings thus point to considerable involvement of acute stress in clearance and/or tissue distribution of IONs associated with alterations in vascular function and BP regulation after a single *i.v.* IONs application.

Acknowledgments: The authors thank Mrs. J. Petova and Mrs. B. Bolgacova for their technical assistance. This research was funded by the research grants APVV-16-0263, VEGA 2/0160/17, APVV-17-0178, and SAV-BAV-18-11.

Conflicts of Interest: The authors declare no conflict of interest.

References

ALMEIDA JP, CHEN AL, FOSTER A, DREZEK R: In vivo biodistribution of nanoparticles. Nanomedicine (Lond) 6: 815-835, 2011.

ANDRADE RGD, VELOSO SRS, CASTANHEIRA EMS: Shape Anisotropic Iron Oxide-Based Magnetic Nanoparticles: Synthesis and Biomedical Applications. Int J Mol Sci 21: 2020.

ASTANINA K, SIMON Y, CAVELIUS C, PETRY S, KRAEGELOH A, KIEMER AK: Superparamagnetic iron oxide nanoparticles impair endothelial integrity and inhibit nitric oxide production. Acta Biomater 10: 4896-4911, 2014.

BARATLI Y, CHARLES AL, WOLFF V, BEN TAHAR L, SMIRI L, BOUITBIR J, ZOLL J, PIQUARD F, TEBOURBI O, SAKLY M, ABDELMELEK H, GENY B: Impact of iron oxide nanoparticles on brain, heart, lung, liver and kidneys mitochondrial respiratory chain complexes activities and coupling. Toxicol In Vitro 27: 2142-2148, 2013.

BEHULIAK M, PINTEROVA M, BENCZE M, PETROVA M, LISKOVA S, KAREN P, KUNES J, VANECKOVA I, ZICHA J: Ca2+ sensitization and Ca2+ entry in the control of blood pressure and adrenergic vasoconstriction in conscious Wistar-Kyoto and spontaneously hypertensive rats. J Hypertens 31: 2025-2035, 2013.

BENCZE M, VAVŘÍNOVÁ A, ZICHA J, BEHULIAK M: Pharmacological Suppression of Endogenous Glucocorticoid Synthesis Attenuated Blood Pressure and Heart Rate Response to Acute Restraint in Wistar Rats. Physiol Res 69: 415-426, 2020.

BENCZE M, BEHULIAK M, VAVRINOVA A, ZICHA J: Broad-range TRP channel inhibitors (2-APB, flufenamic acid, SKF-96365) affect differently contraction of resistance and conduit femoral arteries of rat. Eur J Pharmacol 765: 533-540, 2015.

BERNATOVA I: Endothelial dysfunction in experimental models of arterial hypertension: cause or consequence? Biomed Res Int 2014: 598271, 2014.

BERNATOVA I, BALIS P, GOGA R, BEHULIAK M, ZICHA J, SEKAJ I: Lack of reactive oxygen species deteriorates blood pressure regulation in acute stress. Physiol Res 65: S381-S390, 2016.

BOSTAN HB, REZAEE R, VALOKALA MG, TSAROUHAS K, GOLOKHVAST K, TSATSAKIS AM, KARIMI G: Cardiotoxicity of nano-particles. Life Sci 165: 91-99, 2016.

COURTOIS A, ANDUJAR P, LADEIRO Y, DUCRET T, ROGERIEUX F, LACROIX G, BAUDRIMONT I, GUIBERT C, ROUX E, CANAL-RAFFIN M, BROCHARD P, MARANO F, MARTHAN R, MULLER B: Effect of engineered nanoparticles on vasomotor responses in rat intrapulmonary artery. Toxicol Appl Pharmacol 245: 203-210, 2010.

DALZON B, TORRES A, REYMOND S, GALLET B, SAINT-ANTONIN F, COLLIN-FAURE V, MORISCOT C, FENEL D, SCHOEHN G, AUDE-GARCIA C,

RABILLOUD T: Influences of Nanoparticles Characteristics on the Cellular Responses: The Example of Iron Oxide and Macrophages. Nanomaterials (Basel) 10: 2020.

DE DOMENICO I, ZHANG TY, KOENING CL, BRANCH RW, LONDON N, LO E, DAYNES RA, KUSHNER JP, LI D, WARD DM, KAPLAN J: Hepcidin mediates transcriptional changes that modulate acute cytokine-induced inflammatory responses in mice. J Clin Invest 120: 2395-2405, 2010.

DOBIAS L, PETROVA M, VOJTKO R, KRISTOVA V: Long-term Treatment with Hesperidin Improves Endothelium-dependent Vasodilation in Femoral Artery of Spontaneously Hypertensive Rats: The Involvement of NO-synthase and Kv Channels. Phytother Res 30: 1665-1671, 2016.

DRÁBKOVÁ N, HOJNÁ S, ZICHA J, VANĚČKOVÁ I: Contribution of Selected Vasoactive Systems to Blood Pressure Regulation in Two Models of Chronic Kidney Disease. Physiol Res 69: 405-414, 2020.

DUKHINOVA MS, PRILEPSKII AY, SHTIL AA, VINOGRADOV VV: Metal Oxide Nanoparticles in Therapeutic Regulation of Macrophage Functions. Nanomaterials (Basel) 9: 2019.

EL HADI H, DI VINCENZO A, VETTOR R, ROSSATO M: Relationship between Heart Disease and Liver Disease: A Two-Way Street. Cells 9: 2020.

IVERSEN NK, FRISCHE S, THOMSEN K, LAUSTSEN C, PEDERSEN M, HANSEN PB, BIE P, FRESNAIS J, BERRET JF, BAATRUP E, WANG T: Superparamagnetic iron oxide polyacrylic acid coated gamma-Fe2O3 nanoparticles do not affect kidney function but cause acute effect on the cardiovascular function in healthy mice. Toxicol Appl Pharmacol 266: 276-288, 2013.

KANBAR R, OREA V, CHAPUIS B, BARRES C, JULIEN C: A transfer function method for the continuous assessment of baroreflex control of renal sympathetic nerve activity in rats. Am J Physiol Regul Integr Comp Physiol 293: R1938-R1946, 2007.

KENZAOUI BH, BERNASCONI CC, HOFMANN H, JUILLERAT-JEANNERET L: Evaluation of uptake and transport of ultrasmall superparamagnetic iron oxide nanoparticles by human brain-derived endothelial cells. Nanomedicine (Lond) 7: 39-53, 2012.

KISHI T: Regulation of the sympathetic nervous system by nitric oxide and oxidative stress in the rostral ventrolateral medulla: 2012 Academic Conference Award from the Japanese Society of Hypertension. Hypertens Res 36: 845-851, 2013.

KLUKNAVSKY M, BALIS P, SKRATEK M, MANKA J, BERNATOVA I: (-)-Epicatechin Reduces the Blood Pressure of Young Borderline Hypertensive Rats During the Post-Treatment Period. Antioxidants (Basel) 9: 2020.

KUMAGAI H, OSHIMA N, MATSUURA T, IIGAYA K, IMAI M, ONIMARU H, SAKATA K, OSAKA M, ONAMI T, TAKIMOTO C, KAMAYACHI T, ITOH H, SARUTA T: Importance of rostral ventrolateral medulla neurons in determining efferent sympathetic nerve activity and blood pressure. Hypertens Res 35: 132-141, 2012.

LEE GK, MAHESHRI N, KASPAR B, SCHAFFER DV: PEG conjugation moderately protects adeno-associated viral vectors against antibody neutralization. Biotechnol Bioeng 92: 24-34, 2005.

LISKOVA S, KUNES J, ZICHA J: Nifedipine-sensitive vascular reactivity of femoral arteries in WKY: the effects of pertussis toxin pretreatment and endothelium removal. Physiol Res 56: 663-666, 2007.

LISKOVA S, PETROVA M, KAREN P, BEHULIAK M, ZICHA J: Contribution of Ca(2+)-dependent Cl(-) channels to norepinephrine-induced contraction of femoral artery is replaced by increasing EDCF contribution during ageing. Biomed Res Int 2014: 289361, 2014.

LISKOVA S, PETROVA M, KAREN P, KUNES J, ZICHA J: Effects of aging and hypertension on the participation of endothelium-derived constricting factor (EDCF) in

norepinephrine-induced contraction of rat femoral artery. Eur J Pharmacol 667: 265-270, 2011.

LISKOVA S, PETROVA M, KAREN P, KUNES J, ZICHA J: Influence of calcium-dependent potassium channel blockade and nitric oxide inhibition on norepinephrine-induced contractions in two forms of genetic hypertension. J Am Soc Hypertens 4: 128-134, 2010.

LONGMIRE M, CHOYKE PL, KOBAYASHI H: Clearance properties of nano-sized particles and molecules as imaging agents: considerations and caveats. Nanomedicine (Lond) 3: 703-717, 2008.

MCBRYDE FD, LIU BH, ROLOFF EV, KASPAROV S, PATON JFR: Hypothalamic paraventricular nucleus neuronal nitric oxide synthase activity is a major determinant of renal sympathetic discharge in conscious Wistar rats. Exp Physiol 103: 419-428, 2018.

MEWISSEN MW: Stenting in the femoropopliteal arterial segment. Tech Vasc Interv Radiol 8: 146-149, 2005.

NAKAMOTO M, OHYA Y, SAKIMA A, YAMAZATO M, TAKISHITA S: Azelnidipine attenuates cardiovascular and sympathetic responses to air-jet stress in genetically hypertensive rats. Hypertens Res 30: 359-366, 2007.

NUNES AD, RAMALHO LS, SOUZA AP, MENDES EP, COLUGNATI DB, ZUFELATO N, SOUSA MH, BAKUZIS AF, CASTRO CH: Manganese ferrite-based nanoparticles induce ex vivo, but not in vivo, cardiovascular effects. Int J Nanomedicine 9: 3299-3312, 2014.

OH N, PARK JH: Endocytosis and exocytosis of nanoparticles in mammalian cells. Int J Nanomedicine 9 Suppl 1: 51-63, 2014.

PECHANOVA O, MATUSKOVA J, CAPIKOVA D, JENDEKOVA L, PAULIS L, SIMKO F: Effect of spironolactone and captopril on nitric oxide and S-nitrosothiol formation in kidney of L-NAME-treated rats. Kidney Int 70: 170-176, 2006.

POLLER WC, PIEBER M, BOEHM-STURM P, RAMBERGER E, KARAMPELAS V, MOLLER K, SCHLEICHER M, WIEKHORST F, LOWA N, WAGNER S, SCHNORR J, TAUPITZ M, STANGL K, STANGL V, LUDWIG A: Very small superparamagnetic iron oxide nanoparticles: Long-term fate and metabolic processing in atherosclerotic mice. Nanomedicine 14: 2575-2586, 2018.

PUZSEROVA A, BERNATOVA I: Blood pressure regulation in stress: focus on nitric oxide-dependent mechanisms. Physiol Res 65: S309-S342, 2016.

PUZSEROVA A, KOPINCOVA J, SLEZAK P, BALIS P, BERNATOVA I: Endothelial dysfunction in femoral artery of the hypertensive rats is nitric oxide independent. Physiol Res 62: 615-629, 2013.

RAUCHOVÁ H, PECHÁNOVÁ O, KUNES J, VOKURKOVÁ M, DOBESOVÁ Z, ZICHA J: Chronic N-acetylcysteine administration prevents development of hypertension in N(omega)-nitro-L-arginine methyl ester-treated rats: the role of reactive oxygen species. Hypertens Res 28: 475-482, 2005.

SKRATEK MK, M.; BARTA, A.; BALIS, P.; MICUROVA, A.; DVURECENSKIJ, A.; CIGAN, A.; ECKSTEIN – ANDICSOVA A.; J. MANKA, J.; BERNATOVA, I. : Sensitive SQUID bio-magnetometry for determination and differentiation of biogenic iron and iron oxide nanoparticles in biological samples. Nanomaterials, 2020

SLEZAK P, PUZSEROVA A, BALIS P, SESTAKOVA N, MAJZUNOVA M: Genotype-related effect of crowding stress on blood pressure and vascular function in young female rats. Biomed Res Int 2014: 413629, 2014.

STEFANO GB, FRICCHIONE GL, ESCH T: Relaxation: molecular and physiological significance. Med Sci Monit 12: Hy21-Hy31, 2006.

STOJICIĆ S, MILUTINOVIĆ-SMILJANIĆ S, SARENAC O, MILOSAVLJEVIĆ S, PATON JF, MURPHY D, JAPUNDZIĆ-ZIGON N: Blockade of central vasopressin receptors

reduces the cardiovascular response to acute stress in freely moving rats. Neuropharmacology 54: 824-836, 2008.

SU L, HAN L, GE F, ZHANG SL, ZHANG Y, ZHAO BX, ZHAO J, MIAO JY: The effect of novel magnetic nanoparticles on vascular endothelial cell function in vitro and in vivo. J Hazard Mater 235-236: 316-325, 2012.

SUK JS, XU Q, KIM N, HANES J, ENSIGN LM: PEGylation as a strategy for improving nanoparticle-based drug and gene delivery. Adv Drug Deliv Rev 99: 28-51, 2016.

SUN J, WANG S, ZHAO D, HUN FH, WENG L, LIU H: Cytotoxicity, permeability, and inflammation of metal oxide nanoparticles in human cardiac microvascular endothelial cells: cytotoxicity, permeability, and inflammation of metal oxide nanoparticles. Cell Biol Toxicol 27: 333-342, 2011.

TORTI FM, TORTI SV: Regulation of ferritin genes and protein. Blood 99: 3505-3516, 2002.

VUKOVA TI, DIMITROV SD, GAGOV HS, DIMITROVA DZ: In focus: Fe3O4 nanoparticles and human mesenteric artery interaction in vitro. Nanomedicine (Lond) 11: 921-932, 2016.

WANG J, RAO H, WETMORE GS, FURLAN PM, KORCZYKOWSKI M, DINGES DF, DETRE JA: Perfusion functional MRI reveals cerebral blood flow pattern under psychological stress. Proc Natl Acad Sci U S A 102: 17804-17809, 2005.

WANG YX: Superparamagnetic iron oxide based MRI contrast agents: Current status of clinical application. Quant Imaging Med Surg 1: 35-40, 2011.

WSOL A, WOJNO O, PUCHALSKA L, WRZESIEN R, SZCZEPANSKA-SADOWSKA E, CUDNOCH-JEDRZEJEWSKA A: Impaired hypotensive effects of centrally acting oxytocin in SHR and WKY rats exposed to chronic mild stress. Am J Physiol Regul Integr Comp Physiol 318: R160-r172, 2020.

XIONG F, WANG H, FENG Y, LI Y, HUA X, PANG X, ZHANG S, SONG L, ZHANG Y, GU N: Cardioprotective activity of iron oxide nanoparticles. Sci Rep 5: 8579, 2015.

YAMAZATO M, OHYA Y, NAKAMOTO M, SAKIMA A, TAGAWA T, HARADA Y, NABIKA T, TAKISHITA S: Sympathetic hyperreactivity to air-jet stress in the chromosome 1 blood pressure quantitative trait locus congenic rats. Am J Physiol Regul Integr Comp Physiol 290: R709-714, 2006.

YARJANLI Z, GHAEDI K, ESMAEILI A, RAHGOZAR S, ZARRABI A: Iron oxide nanoparticles may damage to the neural tissue through iron accumulation, oxidative stress, and protein aggregation. BMC Neuroscience 18: 51, 2017.

YOFFE S, LESHUK T, EVERETT P, GU F: Superparamagnetic iron oxide nanoparticles (SPIONs): synthesis and surface modification techniques for use with MRI and other biomedical applications. Curr Pharm Des 19: 493-509, 2013.

ZHANG YN, POON W, TAVARES AJ, MCGILVRAY ID, CHAN WCW: Nanoparticle-liver interactions: Cellular uptake and hepatobiliary elimination. Journal of controlled release : official journal of the Controlled Release Society 240: 332-348, 2016.

ZHU MT, WANG Y, FENG WY, WANG B, WANG M, OUYANG H, CHAI ZF: Oxidative stress and apoptosis induced by iron oxide nanoparticles in cultured human umbilical endothelial cells. J Nanosci Nanotechnol 10: 8584-8590, 2010.

Tables

Table 1. Parameters of endothelium-independent and endothelium-dependent relaxations induced by sodium nitroprusside and acetylcholine, respectively.

Parameter/Group	Cont	IONs	Str	IONs + Str
Sodium nitroprusside–induced relaxations				
EC_{50} (-log mol/l)	8.41 ± 0.04	8.14 ± 0.08*	8.22 ± 0.07	8.10 ± 0.06*
E_{max} (%)	98.30 ± 0.79	99.57 ± 1.28	97.15 ± 1.24	98.60 ± 0.75
Acetylcholine-induced relaxations				
EC_{50} (-log mol/l)	7.58 ± 0.05	7.58 ± 0.12	7.86 ± 0.12	7.48 ± 0.11
E_{max} (%)	92.68 ± 0.94	90.65 ± 1.17	91.01 ± 1.39	92.40 ± 1.05
$EC_{50\ L\text{-}NAME}$ (-log mol/l)	7.11 ± 0.13**	7.03 ± 0.13**	6.98 ± 0.07**	6.89 ± 0.10**
$E_{max\ L\text{-}NAME}$ (%)	85.60 ± 2.40	62.20 ± 6.23**	83.83 ± 2.68	84.28 ± 6.68^{+}
$E_{max\ L\text{-}NAME\text{-}sensitive}$ (%)	7.07 ± 2.59	28.45 ± 6.71*	7.19 ± 2.10	8.11± 6.10^{+}

The values represent the mean ± SEM. *p < 0.05 vs. the control group, **p < 0.05 *vs.* the same parameter without L-NAME, $^{+}$p < 0.05 *vs.* IONs group, n = 6 - 7 per group. Abbreviations. Cont: control group, IONs: rats treated with ultra-small superparamagnetic iron oxide nanoparticles, Str: rats exposed to repeated air-jet stress, IONs + Str: rats treated with nanoparticles and co-exposed to repeated air-jet stress, L-NAME: N^{ω}-nitro-L-arginine methyl ester, EC_{50}: half-maximal effective concentration, $EC_{50\ L\text{-}NAME}$: half-maximal effective concentration in the presence of L-NAME, E_{max}: maximal relaxation, $E_{max\ L\text{-}NAME}$: maximal relaxation in the presence of L-NAME.

Figures Legends

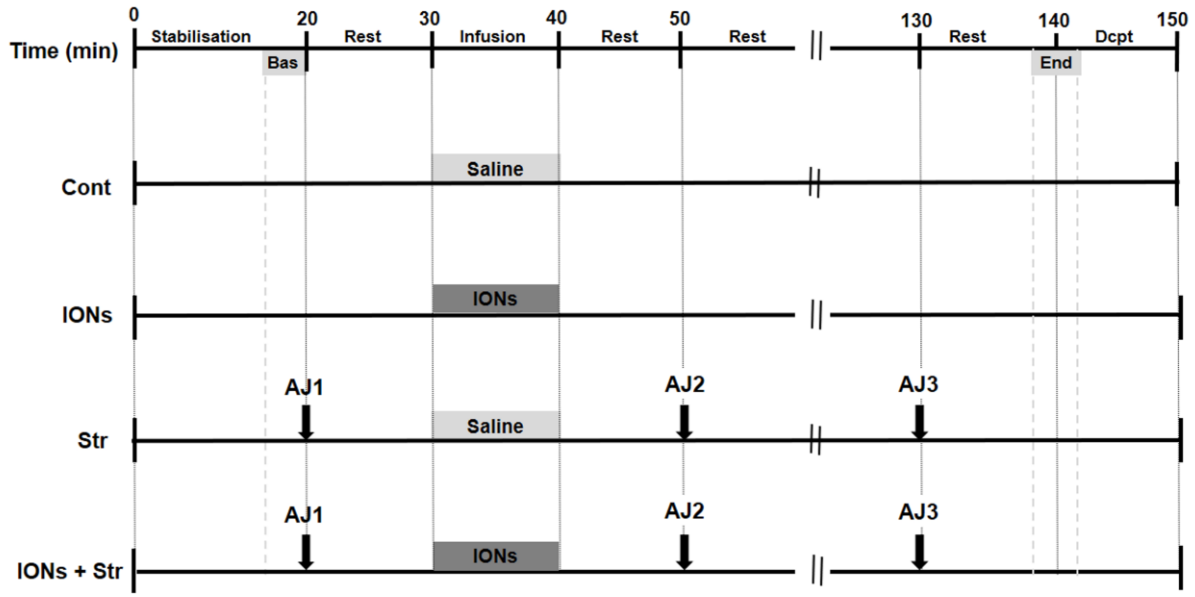

Figure 1. Time course of the experimental protocol. Stress was induced by 5-s air-jets (AJ) as described previously (Bernátová *et al.* 2016). Basal recordings of blood pressure and heart rate were determined at the beginning (Bas) and at the end (End) of the experiment as the average values of approximately 200-sec segments between 16–20 min and 138–142 min of the experiment. Then the animals were decapitated (Dcpt).

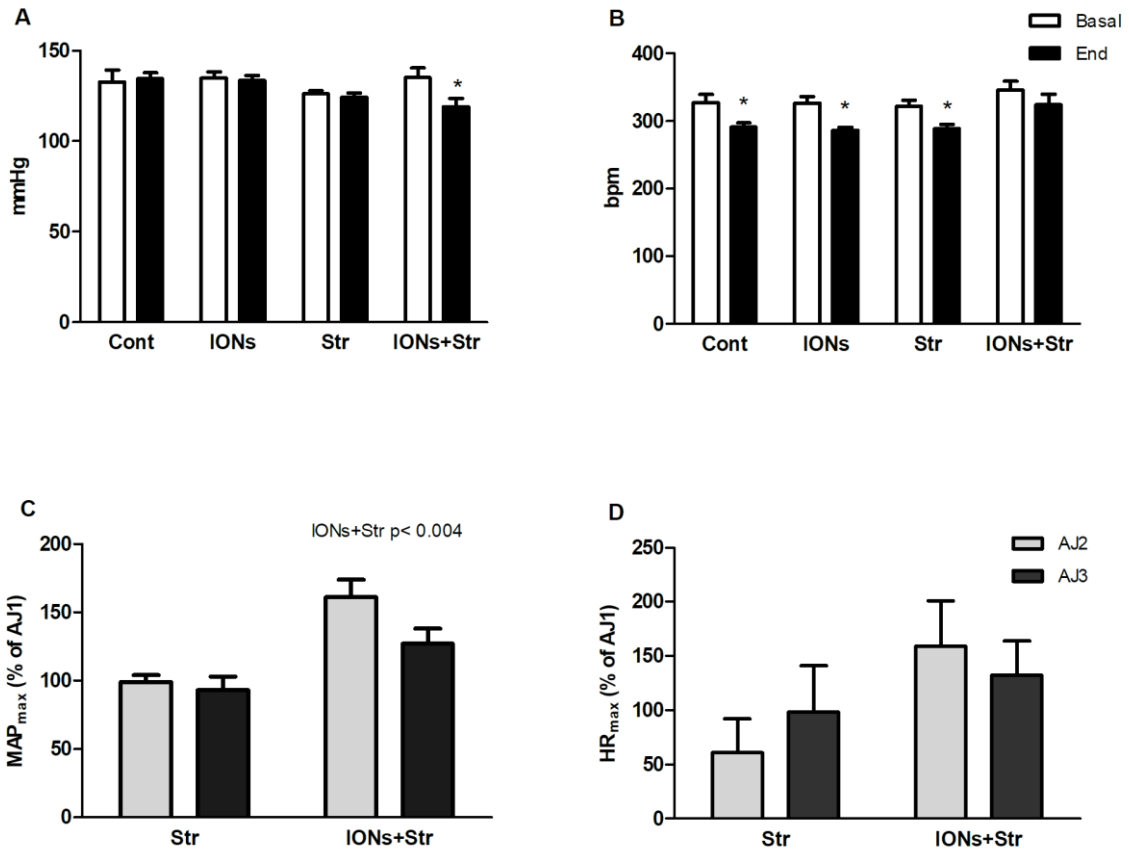

Figure 2. Mean arterial pressure (A) and heart rate (B) at the beginning (basal) and the end of the experiment as well as peak values of mean arterial pressure (C) and heart rate (D) during the second and third air-jet session as a relative value of the first air-jet session. The values represent the mean ± SEM. *$p < 0.05$ *vs.* basal in the respective group (Figures A, B). $p < 0.004$ main effect of IONs + Str vs. Str group (Figure C), n = 6 per group. Abbreviations. AJ: air-jet, Cont: control group, IONs: rats treated with ultra-small superparamagnetic iron oxide nanoparticles, Str: rats exposed to repeated air-jet stress, IONs + Str: rats treated with nanoparticles and co-exposed to repeated air-jet stress.

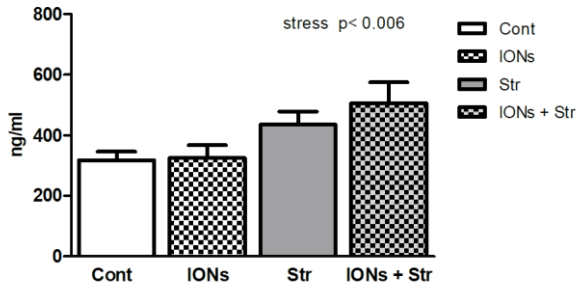

Figure 3. Plasma corticosterone. Stress elevated plasma corticosterone when determined as the main effect of stress. The values represent the mean ± SEM. *p < 0.006 main effect of stress vs. unstressed rats. n = 6 per group. Abbreviations. Cont: control group, IONs: rats treated with ultra-small superparamagnetic iron oxide nanoparticles, Str: rats exposed to repeated air-jet stress, IONs + Str: rats treated with nanoparticles and co-exposed to repeated air-jet stress.

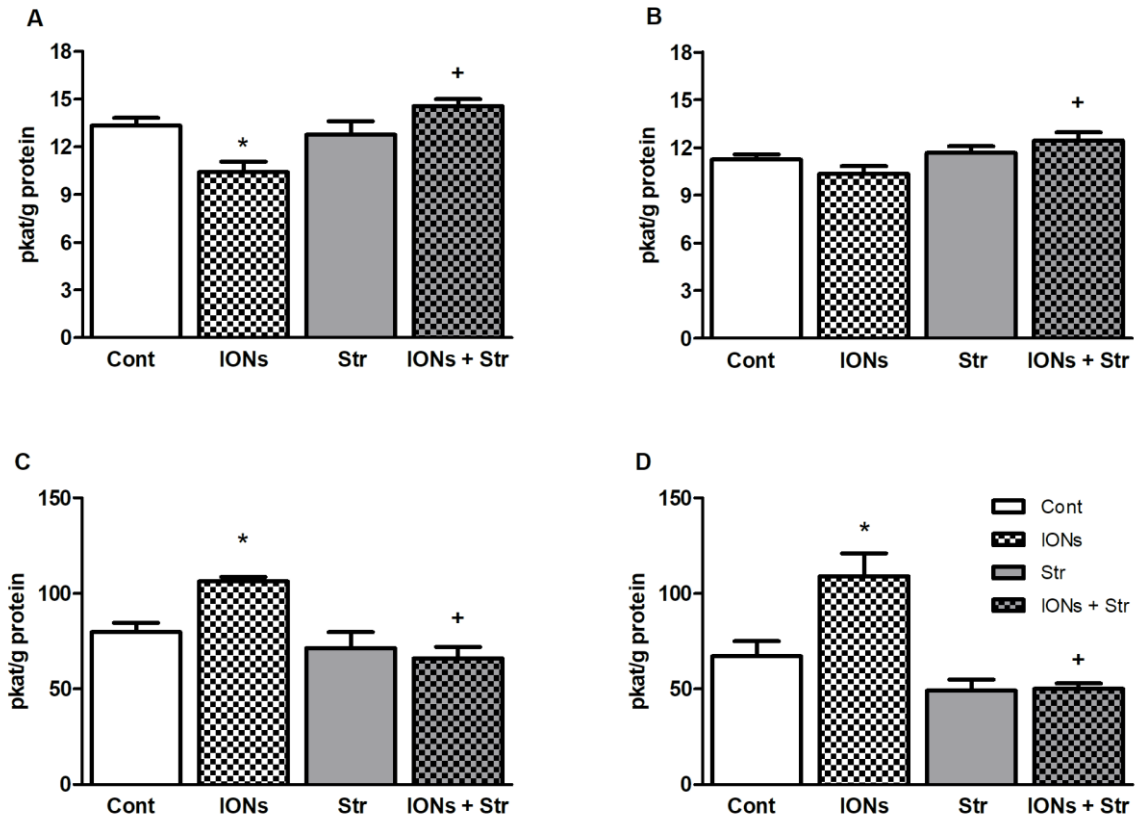

Figure 4. Nitric oxide synthase activity in the kidneys (A), liver (B), hypothalamus (C) and brainstem (D). The values represent the mean ± SEM. *p < 0.05 *vs.* Cont group, $^{+}$p < 0.05 *vs.* IONs group, n = 6 per group. Abbreviations. Cont: control group, IONs: rats treated with ultra-small superparamagnetic iron oxide nanoparticles, Str: rats exposed to repeated air-jet stress, IONs + Str: rats treated with nanoparticles and co-exposed to repeated air-jet stress.

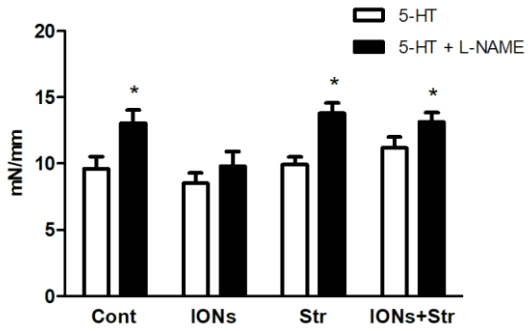

Figure 5. Maximal serotonin (5-hydroxytryptamine)-induced contractions in the absence and presence of NO synthase inhibitor L-NAME. The values represent the mean ± SEM. *$p < 0.05$ *vs.* 5-HT, n = 6 - 7 per group. Abbreviations. Cont: control group, IONs: rats treated with ultra-small superparamagnetic iron oxide nanoparticles, Str: rats exposed to repeated air-jet stress, IONs + Str: rats treated with nanoparticles and co-exposed to repeated air-jet stress, 5-HT: 5-hydroxytryptamine, L-NAME: N^{ω}-nitro-L-arginine methyl ester.

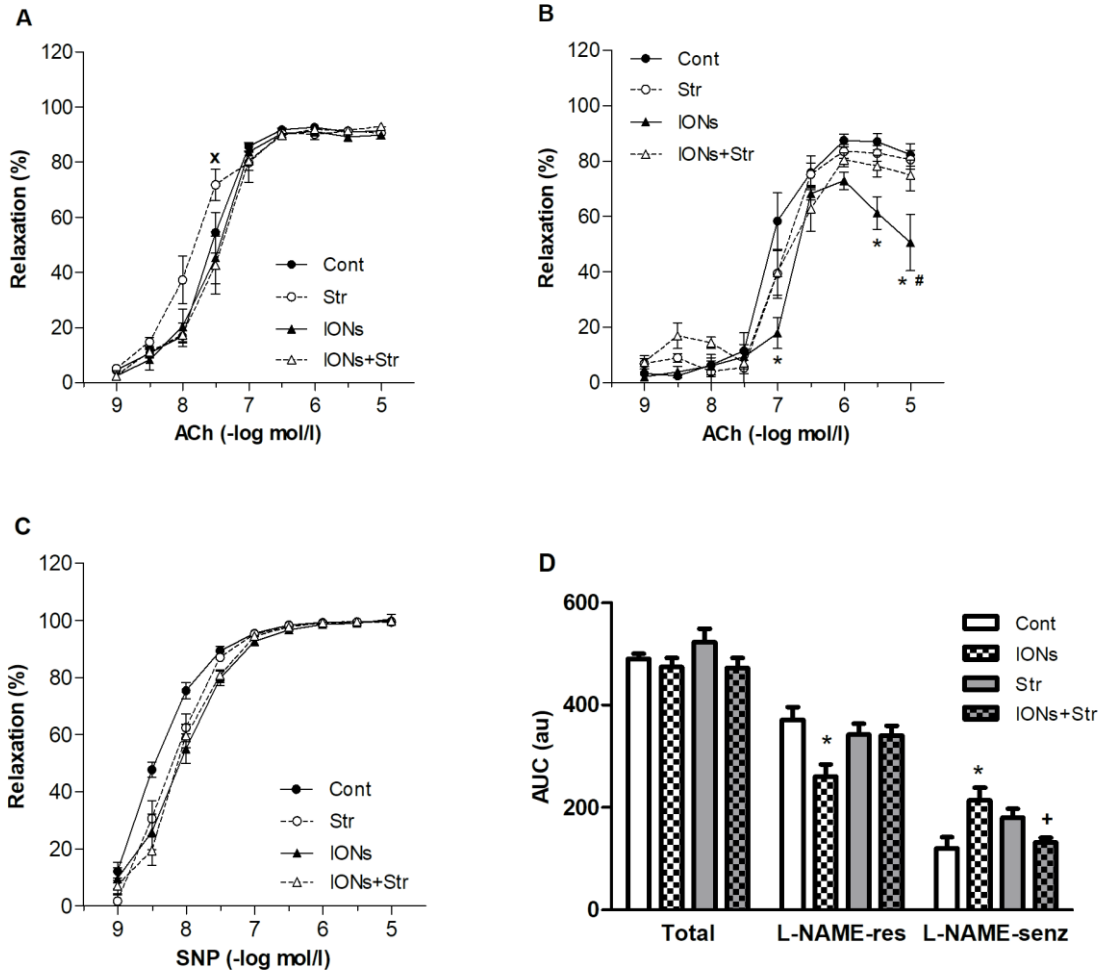

Figure 6. Acetylcholine-induced relaxations in the absence (A) and presence (B) of L-NAME, sodium nitroprusside-induced relaxation (C) and L-NAME-sensitive and L-NAME-resistant components of acetylcholine-induced relaxations (D) in the femoral arteries. The values represent the mean ± SEM, n = 6–7 per group. $^{x}p < 0.001$ *vs.* the IONs + Str group, $*p < 0.05$ *vs.* the same parameter of the control group, $^{\#}p < 0.02$ vs. the maximal relaxation in the IONs group (at ACh concentration 10^{-6} mol/l), $^{+}p < 0.05$ *vs.* the same parameter in the IONs group. Abbreviations. Cont: control group, IONs: rats treated with ultra-small superparamagnetic iron oxide nanoparticles, Str: rats exposed to repeated air-jet stress, IONs + Str: rats treated with nanoparticles and co-exposed to repeated air-jet stress, ACh: acetylcholine, L-NAME: N^{ω}-nitro-L-arginine methyl ester.

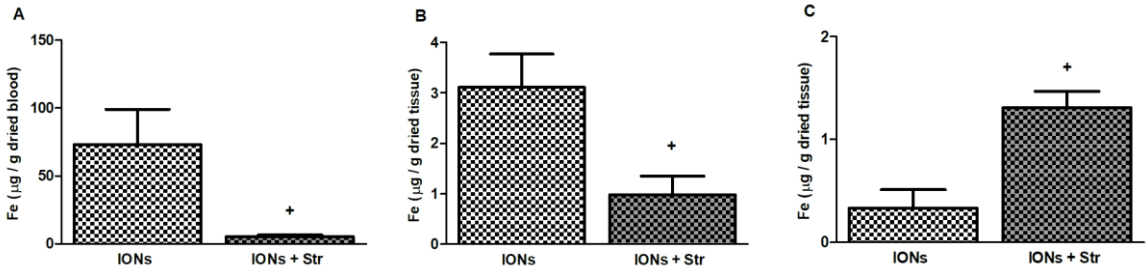

Figure 7. IONs-originated iron content in blood (A), liver (B) and kidney (C) in IONs and IONs +Str groups. The values represent the mean ± SEM, n = 5-6 per group. $^{+}p < 0.04$ *vs.* the IONs group. Abbreviations. IONs: rats treated with ultra-small superparamagnetic iron oxide nanoparticles, IONs + Str: rats treated with nanoparticles and co-exposed to repeated air-jet stress.

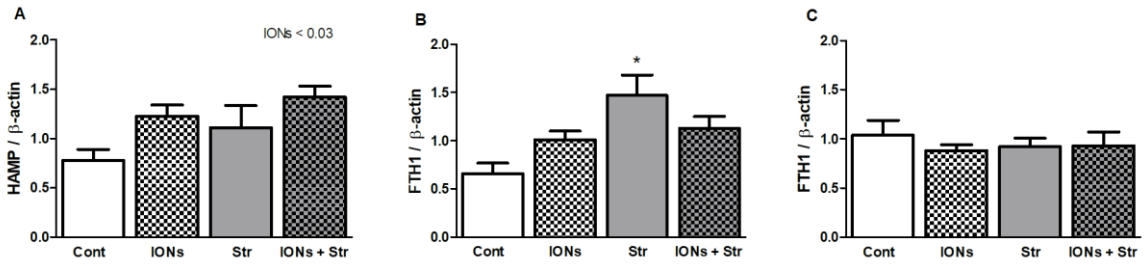

Figure 8. The expression levels of hepcidin gene in the liver (A) and ferritin heavy chain 1 in the liver (B) and kidneys (C). The values represent the mean ± SEM. *$p < 0.006$ *vs* the control group, $p < 0.03$ main effect of IONs vs. ION-untreated groups, n = 5-6 per group. Abbreviations. *HAMP*: hepcidin gene, *FTH1*: ferritin heavy chain 1 gene, Cont: control group, IONs: rats treated with ultra-small superparamagnetic iron oxide nanoparticles, Str: rats exposed to repeated air-jet stress, IONs + Str: rats treated with nanoparticles and co-exposed to repeated air-jet stress.